AIP | Applied Physics Letters

Investigation of optimal hydrogen sensing performance in semiconducting carbon nanotube network transistors with palladium electrodes

Bongsik Choi, Dongil Lee, Jae-Hyuk Ahn, Jinsu Yoon, Juhee Lee, Minsu Jeon, Dong Myong Kim, Dae Hwan Kim, Inkyu Park, Yang-Kyu Choi, and Sung-Jin Choi

Citation: Applied Physics Letters **107**, 193108 (2015); doi: 10.1063/1.4935610
View online: http://dx.doi.org/10.1063/1.4935610
View Table of Contents: http://scitation.aip.org/content/aip/journal/apl/107/19?ver=pdfcov
Published by the AIP Publishing

Investigation of optimal hydrogen sensing performance in semiconducting carbon nanotube network transistors with palladium electrodes

Bongsik Choi,[1,a)] Dongil Lee,[2,a)] Jae-Hyuk Ahn,[3,4,5] Jinsu Yoon,[1] Juhee Lee,[1] Minsu Jeon,[1] Dong Myong Kim,[1] Dae Hwan Kim,[1] Inkyu Park,[3,4] Yang-Kyu Choi,[2,b)] and Sung-Jin Choi[1,b)]
[1]*School of Electrical Engineering, Kookmin University, Seoul 136-702, South Korea*
[2]*Department of Electrical Engineering, KAIST, Daejeon 305-701, South Korea*
[3]*Department of Mechanical Engineering, KAIST, Daejeon 305-701, South Korea*
[4]*Mobile Sensor and IT Convergence Center, KAIST, Daejeon 305-701, South Korea*
[5]*Department of Physics and Astronomy, University of Pennsylvania, Philadelphia, Pennsylvania 19104, USA*

(Received 13 May 2015; accepted 2 November 2015; published online 12 November 2015)

The work function of palladium (Pd) is known to be sensitive to hydrogen (H_2) via the formation of a surface dipole layer or Pd hydride. One approach to detect such a change in the work function is based on the formation of a Schottky barrier between Pd and a semiconductor. Here, we demonstrate a H_2 sensor operable at room temperature by assembling solution-processed, pre-separated semiconducting single-walled carbon nanotube (SWNT) network bridged by Pd source/drain (S/D) electrodes in a configuration of field-effect transistors (FETs) with a local back-gate electrode. To begin with, we observed that the H_2 response of the fabricated SWNT FETs can be enhanced in the linear operating regime, where the change in the work function of the Pd S/D electrodes by H_2 can be effectively detected. We also explore the H_2 responses in various SWNT FETs with different physical dimensions to optimize the sensing performance. © *2015 AIP Publishing LLC*.
[http://dx.doi.org/10.1063/1.4935610]

Hydrogen (H_2) is considered to be one of the most promising clean energy carriers and is essential in various fields of research and industry, such as fuel cells, automobile engines, industrial processing, chemical production, and cryogenic cooling.[1–3] Thus, monitoring H_2 is of paramount importance due to its low ignition energy and its wide range of flammability for safety concerns.[1–3] Today, commercial H_2 sensors are based on electrochemical responses, mass spectrometry, measurement of electrical resistance, and thermal conductivity measurements.[1,2] For mass production, sensors based on measuring the electrical resistance changes are the most attractive because they are easy to miniaturize and integrate into read-out electronics.[1,4] Their central sensing unit can be a field-effect transistor (FET) with hydrogen-sensitive materials, such as platinum (Pt), chrome (Cr), or palladium (Pd).[5–15] Among these materials, Pd has demonstrated a significantly higher sensitivity with outstanding rapidity of responses and recovery times compared with those of other materials.[7]

A Schottky barrier, which forms at the interface between a metal and a semiconductor, could be a useful sensing element in the FET-based sensors because the electrical responses of the sensors can be strongly modulated by modifying the Schottky barrier height (SBH) formed on the work functions of the two materials.[5–8] Therefore, various structures of FET-based sensors with the Schottky barrier created between the Pd and semiconductors have been proposed for monitoring H_2 because during H_2 exposure, the SBH at the interface can be modulated, resulting from the change in the Pd work function by H_2 adsorption.[5–8] Therefore, FET structures using a pre-separated, semiconducting single-walled carbon nanotube (SWNT) channel in contact with a Pd source and drain (S/D) electrodes have been attractive candidates for the structure of a H_2 sensor with a high sensitivity, fast response, low power consumption, and low cost together with the unique and remarkable electrical, physical, mechanical, and chemical properties of SWNTs.[7] Two groups of structures with SWNT FETs have been reported for potential H_2 detection: pristine SWNT FETs with Pd S/D electrodes[7–10] and Pd-coated SWNT FETs.[9–15] It has been generally accepted that Pd-coated SWNT FETs exhibit significant modulation of electrical conductance upon exposure to H_2,[9–15] whereas pristine SWNT FETs with Pd S/D electrodes have demonstrated a relatively lower sensitivity[7,8] or no response at all.[9,10] Yet to date, there have been few systematic studies that address how fundamental factors of SWNT FETs affect their sensitivity. Here, we demonstrate that the H_2 response of a pristine SWNT network based FETs with Pd S/D electrodes for H_2 detection produced from a solution processed, pre-separated, and semiconducting SWNT solution[16–18] can be enhanced in the linear operating regime where the change in the contact resistance (R_c) associated with the change in SBH[19] by H_2 adsorption on Pd S/D electrodes is the most effective due to the decreased channel resistance of the SWNT network channel. We also study the H_2 responses of fabricated SWNT FET sensors with various physical dimensions.

Figure 1(a) shows a schematic of our sensor structure with the SWNT network channel bridged by Pd S/D electrodes. For effective modulation of conductance in a network channel, we used the structure of a local back-gate. First, a highly p-doped silicon wafer with a thermally grown 50-nm thick SiO_2 layer is used as the substrate. To fabricate the local back-gate, a 30-nm thick Pd layer was deposited and

[a)]B. Choi and D. Lee contributed equally to this work.
[b)]Electronic addresses: ykchoi@ee.kaist.ac.kr and sjchoiee@kookmin.ac.kr. Tel.: +82-2-910-5543. Fax: +82-2-910-4449.

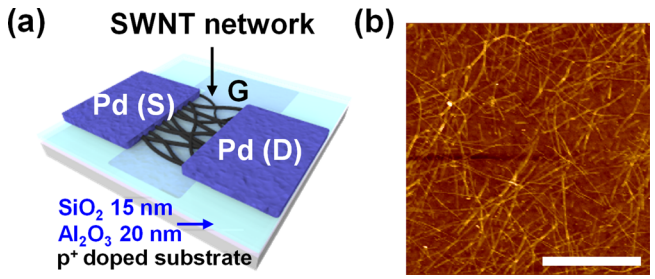

FIG. 1. (a) Device schematic for local back-gate SWNT FET for H_2 sensing. (b) AFM image (z-scale is 10 nm) of an SWNT network constructed with 90% semiconducting SWNT solution with a deposition time of 3 min. Scale bar is 1 μm.

patterned using thermal evaporation and a lift-off process, respectively. Then, a 20-nm thick Al_2O_3 layer was deposited by atomic layer deposition (ALD) as a gate dielectric followed by the deposition of 15-nm thick SiO_2 layer from plasma enhanced chemical vapor deposition (PECVD) to adhere the pre-separated semiconducting SWNTs. Next, after cleaning the surface of the SiO_2 layer, the surface was subsequently functionalized with poly-L-lysine solution (0.1% w/v in water; Sigma Aldrich) to form an amine-terminated layer, which acts as an effective adhesion layer for the SWNTs. To deposit a random network of SWNTs, the SiO_2 surface was immersed for a deposition time of 3 min in a commercially available solution (0.01 mg/ml) of pre-separated semiconducting SWNTs (90% semiconducting from Nanointegris, Inc.). Later, the SiO_2 surface was rinsed with deionized (DI) water and isopropyl alcohol (IPA) and dried with flowing nitrogen. To form S/D electrodes, a 30-nm thick Pd layer was deposited and patterned with thermal evaporation and a lift-off process, respectively. Finally, because the SWNT network film covers the entire wafer, to achieve an accurate channel length (L) and width (W) and to prevent any possible leakage in the devices, an additional photolithography step combined with O_2 plasma was used to remove the unwanted SWNTs outside the channel region. The L and W values of the patterned SWNT network ranged from 1.4 μm to 2.3 μm and 2 μm to 5 μm, respectively. Figure 1(b) shows the atomic force microscopy (AFM) images of the SWNT network channel. The AFM image reveals that the pre-separated semiconducting SWNTs are randomly deposited on the SiO_2 surface. The average SWNT densities obtained with a deposition time of 3 min were found to be 17–24 tubes/μm^2.

First, the transfer and output characteristics of the fabricated pristine local back-gate SWNT FETs were measured in an ambient condition, as shown in Figures 2(a) and 2(b), respectively. The fabricated pristine SWNT FETs normally exhibit p-type behavior in an ambient environment due to the adsorption of oxygen molecules and moisture, and large work function of the Pd material.[20,21] We confirm that the fabricated SWNT FETs with $L = 2.3\ \mu m$ and $W = 2\ \mu m$ with a deposition time of 3 min had a high on/off ratio, exceeding 10^4, which is mostly likely due to the pre-separated semiconducting SWNTs. In addition, the output characteristics appear to be linear for a drain voltage (V_D) between 0 and −0.5 V, which indicates that ohmic contacts at the interface between the Pd and SWNTs were initially

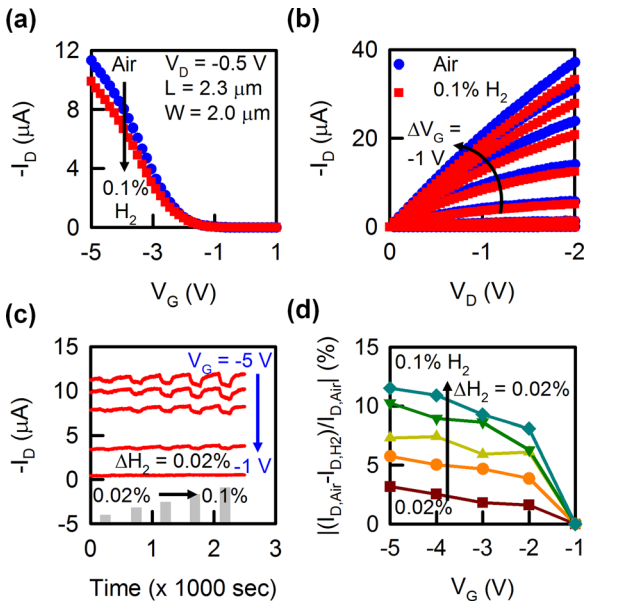

FIG. 2. H_2 response characteristics of the SWNT FET sensor with Pd S/D electrodes at $L = 2.3\ \mu m$ and $W = 2.0\ \mu m$. (a) Transfer characteristics of SWNT FETs in air (blue circle) and 0.1% H_2 gas (red square) ambient ($V_D = -0.5$ V). (b) Output characteristics with various V_G values ranging from 1 to −5 V. (c) Real-time measurement of I_D upon H_2 exposure with different concentrations at various V_G values ($V_D = -0.5$ V). (d) Summary of extracted percentage relative responses from Figure 2(c) for various V_G values.

formed due to the larger work function of Pd compared with that of SWNTs.[7,8,16–18]

For the sensing experiment of H_2 gas, the pristine local back-gate SWNT FET with Pd S/D electrodes was mounted on a vacuum chamber probe station equipped with an electrical probing system and a gas inlet/outlet. The H_2 gas was then injected into the gas inlet by mixing dry synthetic air (79% N_2 and 21% O_2) and 0.1% H_2 gas in the air. The concentration of the H_2 gas was controlled by the flow rate of each gas using mass flow controllers (MFCs), where the total gas flow rate was maintained at 100 sccm. Additionally, the drain current (I_D) of the SWNT FET sensor was measured using an Agilent 4156C, and all of the experiments were performed at room temperature.

The transfer and output characteristics were repeatedly measured after the injection of 0.1% H_2 gas for 3 min, which are also shown in Figures 2(a) and 2(b), respectively. During the H_2 exposure, atomic hydrogen is believed to dissolve into the Pd S/D electrodes, and then, the formation of Pd-H rapidly lowers the electronic work function of Pd[7,9] and creates a Schottky barrier at the interfacial Pd-semiconducting SWNT contact.[7,8] As a result, the decrease in I_D after H_2 exposure is observed in both the transfer and output characteristics because the formation of the SBH at the interface upon H_2 exposure can increase the R_c.[19] Interestingly, we note that the threshold voltage (V_T) extracted from the linear extrapolation method was essentially unchanged under H_2 exposure, and only appreciable changes were observed in the linear regime ($V_G - V_T < V_D$, where V_G is a local back-gate voltage) of the transfer characteristics. In addition, we observed that the low field slope in the output characteristics changed after H_2 exposure, particularly for large V_G, which indicates that the adjustment of V_G is the key parameter to

obtain the high sensitivity of a pristine SWNT FET H_2 sensor.

To further investigate the sensor performance, we performed the transient responses of the SWNT FETs for H_2 under various V_G values. The SWNT FET sensor was sequentially tested with diverse concentrations of H_2 gas from 0.02% to 0.1% with a period of H_2 exposure of 3 min and a period with dried air of 5 min, respectively. Figure 2(c) shows that the I_D decreased with the injection of H_2 gas but increased thereafter with the injection of dried air,[7] which is consistent with the anticipated results from the transfer characteristics. This result indicates that the operation of our sensors is fully reversible.[7] Additionally, the change of I_D also increased as the concentration of H_2 gas increased from 0.02% to 0.1%.[7,8,10–15] Importantly, we observed that in the transient response, the percentage relative responses of the SWNT FET sensor, $|(I_{D,Air} - I_{D,H2})/I_{D,Air}| \times 100$, can be varied according to the different V_G values, as expected previously, and the highest percentage relative responses can be achieved at a large V_G of −5 V, i.e., the linear operating regime of the sensor, which completely contrasts the results of FET-based biosensors and gas sensors.[22,23] Figure 2(d) summarizes the extracted percentage relative responses from the transient responses as a function of V_G values. In FET-based biosensors and gas sensors, the biomolecules and gas molecules can directly modulate the conductance of the channel in the FET-based sensors, which means a high sensitivity can be achieved in the subthreshold regime, where the gating effect of the biomolecules and gas molecules bound on the channel surface is most effective due to the reduced screening of carriers in the channel.[22,23] However, in our SWNT FET H_2 sensor, H_2 can only affect the properties of the Schottky barrier contact produced from the Pd and semiconducting SWNTs,[6–8] whereas the SWNT network-based channel cannot be affected.[9,10]

The total resistance (R_T) in the SWNT FETs is a serial combination of the channel resistance (R_{ch}) and the combined R_c associated with the Pd S/D electrodes.[19] It is generally accepted that SWNT network-based FETs have relatively larger R_{ch}, which is attributed to the large number of nanotube-nanotube junctions caused by the high density of the SWNTs in the network compared with that of single SWNT FETs.[24] Therefore, we expect that the change of R_c due to the formation of the Schottky barrier from the decreased work function of Pd induced by H_2 adsorption is difficult to observe in the SWNT network-based FET sensors. This is because the portion of R_c in R_T is significantly inadequate such that the noticeable change of I_D by the altered R_c from H_2 adsorption onto Pd S/D electrodes cannot easily be observed. However, at the linear operating regime, although the resistance of the junctions generated by nanotubes cannot be decreased by V_G, the R_{ch} can further be lowered by a large V_G, i.e., the portion of R_c in R_T can correspondingly be increased. Therefore, the enhancement of H_2 responses in SWNT network-based FET sensors can be achieved at the linear operating regime.

Next, we investigate the H_2 responses of the SWNT FETs with various physical dimensions. First, we compare the transfer characteristics for SWNT FETs with different L values (1.4 μm and 2.3 μm) but the same W value of 2.0 μm (Figure 3(a)). Note that while the device with a longer L of 2.3 μm has a high on/off ratio, exceeding 10^4, the device with a shorter L of 1.4 μm only has an on/off ratio of less than 10.[16,18] This is primarily attributed to the increased probability of direct source-to-drain transport of carriers by the metallic nanotubes (i.e., the presence of 10% metallic nanotubes in our solution). Using these devices, the transient response is also determined for various concentrations of H_2 under different operating regimes by varying V_G values (Figure 3(b)); the results are summarized in Figure 3(c). It is worthwhile to note that the overall responses for the various concentrations of H_2 increased for the SWNT FET with the shorter L of 1.4 μm (Figure 3(d)). Because R_{ch} decreased due to the shortened L and correspondingly, the portion of R_{ch} in R_T decreased. Therefore, the portion of R_c in R_T increased, which improves the sensing performance. We expect that such an experimental result may provide guidelines for acquiring a high sensitivity when designing an H_2 sensor based on a SWNT FET H_2 sensor by shrinking L. However, it should be noted that the H_2 responses according to the V_G values are almost unchanged (Figure 3(c)). Because the SWNT FET with the shorter L has a weakened V_G dependence (on/off ratio ~ 10), the inefficient control of R_{ch} by varying V_G is expected, which leads to the unchanged responses in the V_G values.

Furthermore, we evaluate the H_2 responses of SWNT FETs for H_2 under different W values (W = 2 μm and 5 μm). The transfer characteristics of the devices are also compared in Figure 4(a). Notably, the on/off ratio in the large W device (W = 5 μm) significantly decreased compared with that in the narrow W device (W = 2 μm), which weakened the V_G dependence because the probability of carrying current from the S to D electrodes by metallic nanotubes is larger in the

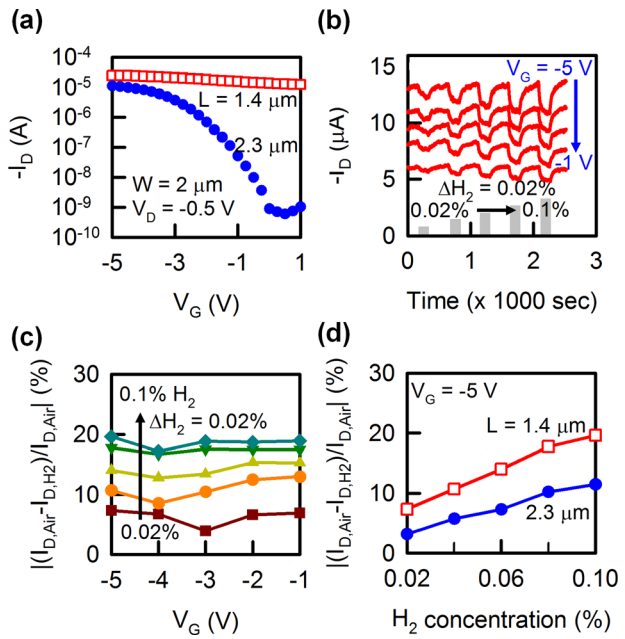

FIG. 3. H_2 response characteristics of the SWNT FET sensors with L = 1.4 μm and 2.3 μm (W is identical for both devices, 2.0 μm). (a) The transfer characteristics of the SWNT FET at L = 1.4 μm (red square) and 2.3 μm (blue circle) at the same W of 2.0 μm. (b) Real-time measurement of I_D upon H_2 exposure with different concentrations at various V_G values with L = 1.4 μm. (c) Summary of extracted percentage relative responses from Fig. 3(b) for various V_G values. (d) Comparison of percentage relative responses for different concentrations of H_2 according to different L values (L = 1.4 μm and 2.3 μm) in SWNT FETs.

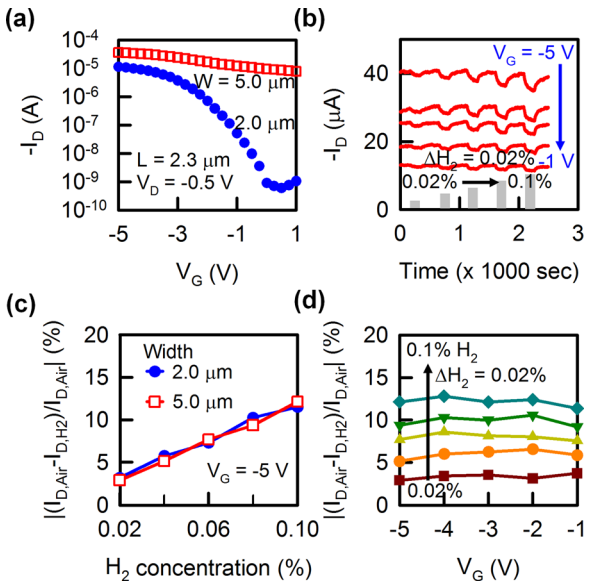

FIG. 4. H_2 response characteristics of the SWNT FET sensors with $W = 2.0\,\mu m$ and $5.0\,\mu m$ (L is identical for both devices, $2.3\,\mu m$). (a) The transfer characteristics of the SWNT FET at $W = 2.0\,\mu m$ (blue circle) and $5.0\,\mu m$ (red square) at the same L of $2.3\,\mu m$. (b) Real-time measurement of I_D upon H_2 exposure with different concentrations at various V_G values with $W = 5.0\,\mu m$. (c) Comparison of percentage relative responses for different concentrations of H_2 according to different W values ($W = 2.0\,\mu m$ and $5.0\,\mu m$) in SWNT FETs. (d) Summary of extracted percentage relative responses from Fig. 4(b) for various V_G values.

large W device.[25] The experimental transient responses for H_2 are shown in Figure 4(b), and the relative responses with the SWNT FETs with different W values are compared in Figure 4(c). Interestingly, the overall relative responses essentially remained unchanged for the device with different W values. For SWNT FETs with $W = 5\,\mu m$, the absolute value of R_c [Ω] decreased in accordance with the expanded contact area contacting the SWNTs with the Pd S/D electrodes, such that it would initially be expected that the sensing performance degrades. However, the R_{ch} also decreased together with decreased R_c by increasing W, which essentially results in the identical proportion of R_c and R_{ch} in R_T. Thus, the same percentage relative responses are obtained between the SWNT FETs with different W values. Moreover, it is worthy to note that the H_2 responses in controlling the V_G value, i.e., adjusting the operating regimes, also remain essentially unchanged due to the weakened V_G dependence (Figure 4(d)), which was similarly explained in the previous case when the results of the different L values were compared.

In conclusion, we have shown that the H_2 response of pristine pre-separated semiconducting SWNT FET with Pd S/D electrodes is enhanced within the linear operating regime. The formation of Pd-H at the Pd-SWNT contacts lowers the work function of Pd, which thus modulates the SBH. We confirmed that the changed R_c as a result of the modulation of SBH by H_2 adsorption is most appreciable in the linear operating regime, i.e., under a large V_G value. Moreover, the H_2 response for the SWNT FETs with various physical dimensions was investigated. The large response was obtained for the pristine SWNT FET with a shorter L value due to the increased portion of R_c in R_T; however, the response remained unchanged between the SWNT FETs with different W values because the portion of R_c cannot be altered effectively. We believe that our work can provide a fundamental understanding regarding the essential guidelines to realize SWNT network-based sensors, particularly for Schottky contact-based sensors. Nevertheless, several hurdles remain. For example, our pristine SWNT FETs exhibited strong dependencies on the electrical characteristics, in particular, the on/off ratio, according to the physical dimensions, such as the L and W values, because we used a low semiconducting enriched nanotube solution (90%). Therefore, a sensitivity study on the SWNT FETs constructed with higher semiconducting enriched solution is important to optimize the sensing performance. Moreover, although the present study focused on the network channel with the same density of SWNTs (deposition time of 3 min), a study on the sensitivity of SWNT FETs with various network densities is necessary because the R_c is also strongly related to the density of the SWNT network.

This work was supported by the National Research Foundation of Korea (NRF) grant funded by the Korea government (Ministry of Education, Science and Technology, MEST) (No. 2013R1A1A1057870) and BK21+ (Educational Research Team for Creative Engineers on Material-Device-Circuit Co-Design).

[1]T. Hubert, L. Boon-Brett, G. Black, and U. Banach, Sens. Actuators, B **157**, 329 (2011).
[2]H. Gu, Z. Wang, and Y. Hu, Sensors **12**, 5517 (2012).
[3]Y. Wang and J. T. W. Yeow, J. Sens. **2009**, 1.
[4]G.-J. Zhang and Y. Ning, Anal. Chim. Acta **749**, 1 (2012).
[5]K. Skucha, Z. Fan, K. Jeon, and A. Javey, Sens. Actuators, B **145**, 232 (2010).
[6]Y. M. Wong, W. P. Kang, J. L. Davidson, A. Wisitsora-at, and K. L. Soh, Sens. Actuators, B **93**, 327 (2003).
[7]M. Zhang, L. L. Brooks, N. Chartuprayoon, W. Bosze, Y.-H. Choa, and N. V. Myung, ACS Appl. Mater. Interfaces **6**, 319 (2013).
[8]A. Javey, J. Guo, Q. Wang, M. Lundstrom, and H. Dai, Nature **424**, 654 (2003).
[9]V. R. Khalap, T. Sheps, A. A. Kane, and P. G. Collins, Nano Lett. **10**, 896 (2010).
[10]J. Sippel-Oakley, H.-T. Wang, B. S. Kang, Z. Wu, F. Ren, A. G. Rinzler, and S. J. Pearton, Nanotechnology **16**, 2218 (2005).
[11]J. Kong, M. G. Chapline, and H. Dai, Adv. Mater. **13**, 1384 (2001).
[12]Y. Sun and H. H. Wang, Adv. Mater. **19**, 2818 (2007).
[13]S. Mubeen, T. Zhang, B. Yoo, M. A. Deshusses, and N. V. Myung, J. Phys. Chem. C **111**, 6321 (2007).
[14]Y. Sun, H. H. Wang, and M. Xia, J. Phys. Chem. C **112**, 1250 (2008).
[15]W. Wongwiriyapan, Y. Okabayashi, S. Minami, K. Itabashi, T. Ueda, R. Shimazaki, T. Ito, K. Oura, S. Honda, H. Tabata, and M. Katayama, Nanotechnology **22**, 055501 (2011).
[16]C. Wang, J. Zhang, K. Ryu, A. Badmaev, L. G. D. Arco, and C. Zhou, Nano Lett. **9**, 4285 (2009).
[17]S.-J. Choi, P. Bennett, K. Takei, C. Wang, C. C. Lo, A. Javey, and J. Boker, ACS Nano **7**, 798 (2012).
[18]S.-J. Choi, C. Wang, C. C. Lo, P. Bennett, A. Javey, and J. Bokor, Appl. Phys. Lett. **101**, 112104 (2012).
[19]S. M. Sze and K. K. Ng, *Physics of Semiconductor Devices* (John Wiley & Sons, Inc., 2007), pp. 187–191.
[20]A. Javey, R. Tu, D. B. Farmer, J. Guo, R. G. Gordon, and H. Dai, Nano Lett. **5**, 345 (2005).
[21]Z. Chen, J. Appenzeller, J. Knoch, Y.-M. Lin, and P. Avouris, Nano Lett. **5**, 1497 (2005).
[22]X. P. A. Gao, G. Zheng, and C. M. Lieber, Nano Lett. **10**, 547 (2010).
[23]J.-H. Ahn, J. Yun, Y.-K. Choi, and I. Park, Appl. Phys. Lett. **104**, 013508 (2014).
[24]J.-W. Do, D. Estrada, X. Xie, N. N. Chang, J. Mallek, G. S. Girolami, J. A. Rogers, E. Pop, and J. W. Lyding, Nano Lett. **13**, 5844 (2013).
[25]Q. Cao, H.-S. Kim, N. Pimparkar, J. P. Kulkarni, C. Wang, M. Shim, K. Roy, M. A. Alam, and J. A. Rogers, Nature **454**, 495 (2008).